

# The 21-cm BAO signature of enriched low-mass galaxies during cosmic reionization

Aviad Cohen<sup>1\*</sup>, Anastasia Fialkov<sup>2,3</sup>, Rennan Barkana<sup>1,4,5</sup>

<sup>1</sup> *Raymond and Beverly Sackler School of Physics and Astronomy, Tel Aviv University, Tel Aviv 69978, Israel*

<sup>2</sup> *Département de Physique, Ecole Normale Supérieure, CNRS, 24 rue Lhomond, Paris, 75005 France*

<sup>3</sup> *Institute for Theory and Computation, Harvard University, 60 Garden Street, MS – 51, Cambridge, MA, 02138 U.S.A.*

<sup>4</sup> *Sorbonne Universités, Institut Lagrange de Paris (ILP), Institut d’Astrophysique de Paris, UPMC Univ Paris 06/CNRS, 98 bis Boulevard Arago, 75014 Paris, France*

<sup>5</sup> *Department of Astrophysics, University of Oxford, Denys Wilkinson Building, Keble Road, Oxford OX1 3RH, UK*

20 January 2021

## ABSTRACT

Studies of the formation of the first stars have established that they formed in small halos of  $\sim 10^5 - 10^6 M_\odot$  via molecular hydrogen cooling. Since a low level of ultraviolet radiation from stars suffices to dissociate molecular hydrogen, under the usually-assumed scenario this primordial mode of star formation ended by redshift  $z \sim 15$  and much more massive halos came to dominate star formation. However, metal enrichment from the first stars may have allowed the smaller halos to continue to form stars. In this Letter we explore the possible effect of star formation in metal-rich low-mass halos on the redshifted 21-cm signal of neutral hydrogen from  $z = 6 - 40$ . These halos are significantly affected by the supersonic streaming velocity, with its characteristic baryon acoustic oscillation (BAO) signature. Thus, enrichment of low-mass galaxies can produce a strong signature in the 21-cm power spectrum over a wide range of redshifts, especially if star formation in the small halos was more efficient than suggested by current simulations. We show that upcoming radio telescopes can easily distinguish among various possible scenarios.

**Key words:** galaxies: formation – galaxies: high redshift – intergalactic medium – cosmology: theory

## 1 INTRODUCTION

The first generation of stars is thought to have formed out of pristine gas via radiative cooling of molecular hydrogen,  $H_2$ , in halos with mass above  $\sim 10^5 M_\odot$  (e.g., Tegmark et al. 1997; Bromm et al. 2002; Yoshida et al. 2003). Radiative cooling of atomic hydrogen (and helium) could only happen in the rarer halos that were heavier than  $\sim 3 \times 10^7 M_\odot$ , corresponding to virial temperatures above  $\sim 10^4$  K (e.g., Barkana & Loeb 2001).

Radiation emitted by the first stars likely had a dramatic impact on subsequent star formation (SF). In particular, photons in the Lyman-Werner (LW) band dissociated  $H_2$  and suppressed SF (Haiman et al. 1997). Simulations have confirmed that, in the presence of LW radiation, the minimum mass of a halo in which primordial gas can radiatively cool increases (Machacek et al. 2001; Wise & Abel 2007; O’Shea & Norman 2008; Visbal et al. 2014). This has moti-

vated the usually-assumed paradigm that SF in molecular-cooling halos was significantly suppressed at  $z \sim 20 - 25$  and completely cut off at  $z \sim 10 - 15$  (Ahn et al. 2009; Holzbauer & Furlanetto 2012; Fialkov et al. 2013), with the more massive atomic-cooling halos likely taking over SF during the early stages of cosmic reionization.

SF in low-mass halos has major observational implications. In general, the most promising probe of early galaxies is the redshifted 21-cm line of neutral hydrogen (e.g., Pritchard & Loeb 2012). The brightness temperature of the 21-cm signal depends on SF through the environmental effects of radiative backgrounds (Lyman- $\alpha$ , X-ray, and ionizing, in particular). Efforts to detect this signal are underway in low-frequency radio observatories whose main focus at present is to probe mid-to-late reionization ( $z \sim 6 - 12$ ) (e.g., van Haarlem 2013; Bowman et al. 2013; Ali et al. 2015), while future experiments are being designed to probe the signal from even higher redshifts (Mellema et al. 2013).

A particularly important effect on small halos is the supersonic streaming velocity of baryons rel-

\* E-mail: aviadc11@gmail.com

ative to the cold dark matter, often referred to as  $v_{bc}$  (Tseliakhovich & Hirata 2010). The baryonic wind suppresses gas infall and SF in  $\sim 10^6 M_\odot$  halos (e.g., Tseliakhovich & Hirata 2010; Dalal et al. 2010; Tseliakhovich et al. 2011; Maio et al. 2011; Stacy et al. 2011; Greif et al. 2011; Fialkov et al. 2012; O’Leary & McQuinn 2012; Naoz et al. 2013; Fialkov 2014). The power spectrum of relative velocity exhibits a strong signature of baryon acoustic oscillations (BAOs) that were imprinted in the velocity field at recombination. Through the effect of  $v_{bc}$  on SF, the BAOs are inherited by the spatial distribution of stars (Dalal et al. 2010; Visbal et al. 2012). This signature, potentially detectable in 21-cm fluctuations, is expected to remain only as long as small halos (well below the atomic-cooling threshold) contribute significant SF.

Depending on their masses, the first generation of metal-free (Pop III) stars ended their lives either via supernova explosions or by direct collapse to a black hole (Woosley & Heger 2015). If a star died in an explosion, metals produced in its core were flung out into its parent galaxy and diffused into the surrounding intergalactic medium. A single explosion was likely enough to raise the gas metallicity within a significant volume above the critical level,  $Z_{\text{crit}} \sim 10^{-4} Z_\odot$ , at which metal-line cooling becomes efficient (Karlsson et al. 2013). Since metals allow cooling down to temperatures as low as  $\text{H}_2$  cooling (and even lower), early metal enrichment suggests a way to avoid the above-mentioned scenario in which small halos become irrelevant at quite high redshifts. Unlike molecular cooling in halos of similar masses, metal cooling is not strongly affected by the LW radiation. Thus, even when the LW background builds up, these halos can continue to form stars. The process that *does* eventually sterilize these light halos is photoheating feedback (e.g., Rees 1986; Weinberg et al. 1997; Navarro & Steinmetz 2000; Sobacchi & Mesinger 2013); once stars emit ionizing radiation, the intergalactic gas that is photoheated above  $10^4$  K stops accreting onto halos below  $\sim 10^8 - 10^9 M_\odot$ , thus quenching subsequent SF within them.

While the details of Pop III stellar evolution and of metallicity dispersal and clumping are complex and uncertain, recent simulations (Wise et al. 2014; Jeon et al. 2014) boost this novel scenario. These numerical studies of early chemical feedback found that metal-enriched SF in halos down to  $M \sim 10^6 M_\odot$  can account for  $\sim 30\%$  of the ionizing photon budget of reionization. Motivated by the possibility of avoiding LW feedback via metal cooling, in this Letter we explore the 21-cm signatures of SF that continues in low-mass halos until reionization.

## 2 MODEL AND METHODS

We use a semi-numerical simulation (Visbal et al. 2012) to follow the non-linear evolution of the 21-cm signal in a  $(768 \text{ Mpc})^3$  volume with  $(3 \text{ Mpc})^3$  cells. We start from a random realization of the initial density and velocity fields, with standard cosmological parameters (Ade et al. 2013). A sub-grid model yields SF and the resulting radiation from each cell. Integration over sources yields the inhomogeneous backgrounds of X-ray,  $\text{Ly}\alpha$  and ionizing radiation, and the resulting 21-cm intensity.

In order to include the photoheating feedback on SF, we begin with the simulation-based formula of Sobacchi & Mesinger (2013) for the minimum halo mass  $M_{\text{crit}}$  that allows significant gas accretion within an ionized region:

$$M_{\text{crit}} = M_0 J_{21}^a \left( \frac{1+z}{10} \right)^b \left[ 1 - \left( \frac{1+z}{1+z_{\text{IN}}} \right)^c \right]^d, \quad (1)$$

a function of redshift  $z$ , the intensity  $J_{21}$  of ionizing radiation<sup>1</sup> in units of  $10^{-21} \text{ erg s}^{-1} \text{ Hz}^{-1} \text{ cm}^{-2} \text{ sr}^{-1}$ , the redshift  $z_{\text{IN}}$  at which the region was reionized, and the parameters  $(M_0, a, b, c, d) = (2.8 \times 10^9 M_\odot, 0.17, -2.1, 2, 2.5)$ .

Eq. (1) considers the effect of feedback on a fully-ionized volume only, while in our simulation some cells are partially ionized by internal sources. We thus modify the prescription of Sobacchi & Mesinger (2013) to more realistically include the feedback on partially ionized cells. At any given redshift  $z$ , we set  $z_{\text{IN}}$  to be the redshift at which the ionization fraction in the cell first passed half of its current value at  $z$ . This improved prescription strengthens feedback and delays reionization by  $\Delta z \sim 1$ . We note that in scenarios in which low-mass halos form stars up until their region is reionized, the large gap between the characteristic halo masses of metal cooling ( $10^6 M_\odot$ ) and of photoheating feedback ( $M_0 = 2 \times 10^9 M_\odot$ ) results in extreme, sudden photoheating feedback that must be computed precisely.

In our simulation a halo forms stars if it is heavy enough to both radiatively cool its gas and resist photoheating feedback. Hence, the minimum halo mass for SF is  $M_{\text{min}} = \max[M_{\text{cool}}, M_{\text{crit}}]$ . A typical cell in our simulation begins with  $z = z_{\text{IN}}$  and  $M_{\text{crit}} = 0$ . Thus,  $M_{\text{min}} = M_{\text{cool}}$ , until reionization of the cell proceeds enough that the difference between  $z_{\text{IN}}$  and  $z$  increases until  $M_{\text{crit}}$  exceeds  $M_{\text{cool}}$ , leading to  $M_{\text{min}} = M_{\text{crit}}$ .  $M_{\text{min}}$  is used to determine the fraction of gas in star-forming halos,  $f_{\text{gas}}$  (Tseliakhovich et al. 2011). For a partially ionized cell,

$$f_{\text{gas}} = f_{\text{gas,neut}}(1 - x_{\text{ion}}) + f_{\text{gas,ion}}x_{\text{ion}}, \quad (2)$$

where  $x_{\text{ion}}$  is the ionized fraction of the cell,  $f_{\text{gas,neut}}$  is the star-forming gas fraction in this cell assuming no photoheating feedback and  $f_{\text{gas,ion}}$  is the same fraction with the feedback. In addition, the effective  $M_{\text{cool}}$  increases in regions with non-zero  $v_{bc}$  (Fialkov et al. 2012).

Metal cooling in low-mass early halos has not been numerically investigated as systematically as the case of molecular cooling, plus it is in any case far more uncertain due to the additional dependence on the production and dispersal of metals. We conservatively assume that metal cooling occurs in the same halos as  $\text{H}_2$  cooling (i.e., down to a circular velocity of  $4.2 \text{ km s}^{-1}$ ), although metal cooling can occur at even lower temperatures. One possible difference between the two cooling channels is the mass dependence of the SF efficiency  $f_*(M)$  at the low-mass end. For  $\text{H}_2$  cooling, we assume a gradual low-mass cutoff as assumed by Fialkov et al.

<sup>1</sup> Noting that  $a$  is small and  $J_{21}$  depends only weakly on redshift (Fig. 7 of Sobacchi & Mesinger (2013)), we simply set  $J_{21} = 0.5$ .

(2013) based on simulations (Machacek et al. 2001):

$$f_*(M) = \begin{cases} f_* & M_{\text{atomic}} < M, \\ f_* \frac{\log(M/M_{\text{min}})}{\log(M_{\text{atomic}}/M_{\text{min}})} & M_{\text{min}} < M < M_{\text{atomic}}, \\ 0 & \text{otherwise,} \end{cases} \quad (3)$$

where  $f_*$  is the efficiency (assumed constant) above the minimum halo mass for atomic cooling,  $M_{\text{atomic}}$ . However, this is not expected to apply to metal cooling. Thus, we also consider a simple, sharp cutoff at  $M_{\text{min}}$ , with a constant SF efficiency  $f_*$  at all  $M > M_{\text{min}}$ . We note that even in the  $\text{H}_2$  cooling case, the applicability of Eq. (3) is quite uncertain since it is based on simulations that are far from demonstrating numerical and physical convergence. In addition, the value of  $f_*$  is highly unconstrained. Some observations suggest a decreasing SF efficiency in metal-poor galaxies (Shi et al. 2014), which may be consistent with low  $f_*$  values in simulations (Jeon et al. 2014; Wise et al. 2014; O’Shea et al. 2015) due to the overall effect of supernovae and radiative feedbacks. We adopt  $f_* \sim 5\%$  as a typical efficiency.

We wish to compare to a model that is based closely on current simulations. O’Shea et al. (2015) presented a fitting function for the fraction of halos containing metal-enriched stars at the final redshift of their simulations,  $f_{\text{occ}}(M)$  (the halo occupancy fraction). This formula implies that halos below  $\sim 10^7 M_{\odot}$  contain almost no stars. Based on the results of Wise et al. (2014) (see their Figure 3), we adopt a smooth transition from high occupancy to the  $f_{\text{occ}}(M)$  formula at redshifts for which the reionization fraction goes from  $\sim 1\%$  to  $\sim 15\%$ . Based on the simulations, in this case we also adopt a low SF efficiency of 0.6%.

It is important to note that current simulations are limited by resolution, given that  $\sim 500$  particles per halo are needed in order to determine overall halo properties (such as halo mass) to within a factor of two (Springel & Hernquist 2003); for better accuracy or to determine properties such as SF, more particles are required. In Wise et al. (2014) and O’Shea et al. (2015), the mass of a 500-particle halo is  $9 \times 10^5 M_{\odot}$  and  $1.4 \times 10^7 M_{\odot}$ , respectively. Simulations with much higher dark matter resolution (Jeon et al. 2015) find some (low-efficiency) SF in halos down to  $10^6 M_{\odot}$  at relatively low redshifts, though such simulations can only follow a tiny cosmic volume that is not representative. Some of our models below assume significantly more SF than is suggested by current simulations; our goal is to show that upcoming observations can easily distinguish among these various possibilities.

Another high-redshift process that is poorly constrained is heating. The spectral energy distribution (SED) of high- $z$  X-ray sources is often modeled by a soft power-law spectrum (Furlanetto 2006). However, the spectrum of X-ray binaries, the known source population most likely to dominate high-redshift X-rays, is expected to be rather hard (Fragos et al. 2013). Illuminated by the hard (compared to soft) X-rays, the Universe heats up more slowly and uniformly, with the heating transition (defined as the time when the mean gas temperature equals that of the cosmic microwave background) delayed due to the larger mean free path of the hard X-ray photons (Fialkov et al. 2014).

### 3 RESULTS

We show predictions for the 21-cm power spectrum (PS) in a number of scenarios, comparing various possibilities including significant metal cooling in small halos. We consider large scales that are feasible to observe and include the characteristic scale of  $\sim 120$  Mpc of the BAO signature from  $v_{\text{bc}}$ . We cover a wide range of redshifts and cosmic events, exploring how the possibility of metal cooling increases the range of possible 21-cm signals compared to previous expectations.

In order to survey the parameter space and isolate various effects (see section 2), we compare six models/cases:

- Our “Maximal” case: hard X-ray SED, sharp  $f_*(M)$  cutoff (i.e., constant  $f_*$  down to  $M_{\text{min}}$ ), with photoheating feedback. This exemplifies a case with effective metal-cooling but ineffective stellar feedback, allowing efficient SF in halos as small as the minimum halo mass for  $\text{H}_2$  cooling.
- The “Simulation-Based” case: Like the Maximal, except with the smooth transition to  $f_{\text{occ}}(M)$  and a ten times lower SF efficiency. This case represents current simulation results.
- The “Gradual” case: Like the Maximal, except with a gradual cutoff in  $f_*(M)$  (Eq. 3). For the metal-cooling case, this illustrates some of the range of uncertainty in the effectiveness of SF in small halos; it also corresponds to the case of  $\text{H}_2$  cooling in the limit of ineffective LW feedback.
- The “No-Feedback” case: Like the Maximal, but without photoheating feedback. This is a comparison case, useful for isolating the effect of photoheating feedback.
- The “Soft” case: Like the Maximal, except with a soft X-ray SED. This case illustrates the effect of one of the key uncertain parameters, the spectrum of early X-ray sources.
- The “Atomic” case: Like the Maximal, but assuming star formation only in halos above the minimum mass for atomic cooling. This is the limiting case of ineffective SF in small halos due to LW or internal feedback; it provides a comparison case for highlighting the impact of small halos.

For each model the SF efficiency is normalized so that the escape fraction of ionizing photons is  $\sim 20\%$  and the total optical depth to reionization is  $\tau = 0.066$  (Ade et al. 2015) (except for the Simulation-Based case, in which we set  $f_* = 0.006$  and assume the resulting required ionizing efficiency). If with this choice of  $f_*$  reionization ends too late, we set it to yield a reionization fraction of at least 95% by  $z = 6$ , while making sure that the optical depth is within the  $2\text{-}\sigma$  error bars of *Planck* (Ade et al. 2015).

Since the streaming velocity causes the most interesting observational signature of small halos, we compare the predictions of each model including or excluding the effect of  $v_{\text{bc}}$ . The effect of  $v_{\text{bc}}$  is expected to be stronger in models with weak feedback, where stars form efficiently in small halos. This effect should thus decrease in the following order: No-Feedback, Maximal/Soft, Gradual, Simulation-Based and Atomic.

We begin by showing the overall redshift evolution of large-scale power (on the BAO scale) in Figure 1, for our six cases with or without the streaming velocity. The comparison among the various cases is made more complex by the fact that a number of distinct sources of 21-cm fluctuations contribute at various times, and also the models are normalized based on observational limits at mid-to-late reionization (i.e., at the low-redshift end of the fig-

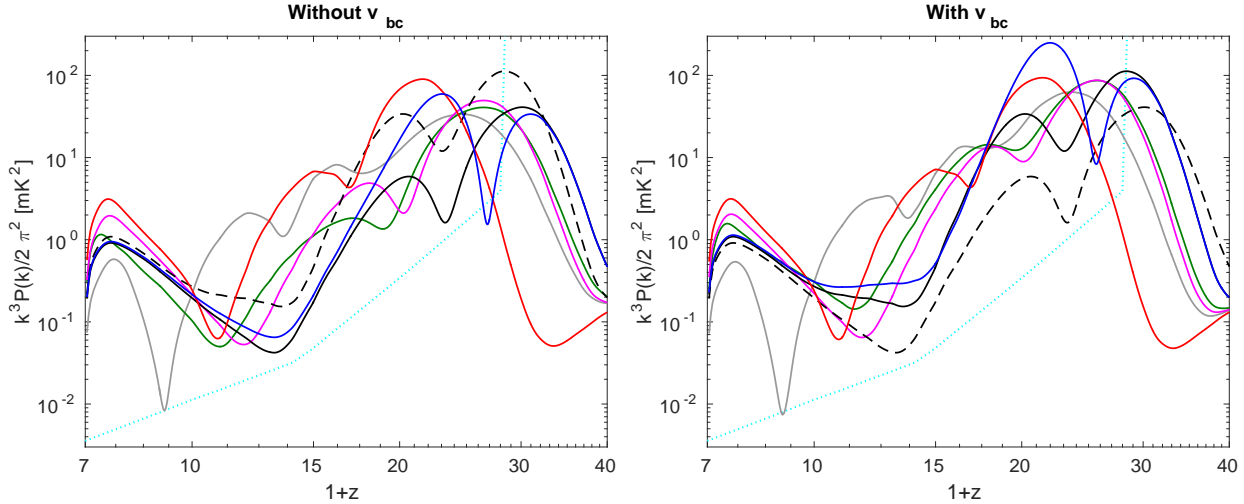


**Figure 1.** The (spherically-averaged) 21-cm power spectrum as a function of redshift. We show the amplitude at  $k = 0.05 \text{ Mpc}^{-1}$  with (right panel) or without (left panel)  $v_{bc}$ . We consider our Maximal (black solid), Simulation-Based (gray), Gradual (magenta), No-Feedback (green), Soft (blue), or Atomic (red) models. For easier comparison, in each panel we also show the PS for the Maximal case from the other panel (black dashed). The cyan dotted line shows the power spectrum of the thermal noise for the SKA1 assuming a single beam, integration time of 1000 hours, and 10 MHz bandwidth.

ure). A generic plot of this type for the 21-cm PS has three peaks (Barkana & Loeb 2005; Pritchard & Furlanetto 2007; Pritchard & Loeb 2008): the high-redshift peak, at  $z \sim 20 - 30$ , is due to Ly $\alpha$  fluctuations; the mid-redshift peak, at  $z \sim 15 - 22$ , is due to heating fluctuations; and the low-redshift peak, at  $z \sim 7$  in these models, is due to ionization fluctuations.

Without  $v_{bc}$ , models with more massive halos have stronger 21-cm fluctuations, since such halos are more strongly biased, and show lower-redshift peaks, since such halos form later. This can be seen by comparing the Atomic, Gradual, and Maximal cases. The streaming velocity has almost no effect on the Atomic case, but greatly enhances the large-scale clustering of small halos, thus lifting the peaks in the Gradual and Maximal cases to the same level as the Atomic case (for the Ly $\alpha$  peak) or even higher (for the heating peak). We note that the increased clustering (due to the spatial fluctuations in  $v_{bc}$ ) is added on top of the increased bias (due to the overall  $v_{bc}$ -induced suppression of SF in low-mass halos).

In the Simulation-Based case all features of the power spectrum are shifted toward lower redshifts compared to the Maximal model due to the slower build-up of stellar populations. For this case there is an extra peak at  $z \sim 14$  due to the transition to very low SF efficiency in small halos (though this added feature is sensitive to the assumed speed of this transition). In addition, fluctuations during reionization are significantly suppressed since the much lower SF efficiency results in colder reionization (for a fixed X-ray to SF efficiency ratio). By comparing to the Maximal case, it can be seen that there is an amplification of the fluctuations due to the  $v_{bc}$  at high redshifts, while at redshifts lower than  $\sim 14$  the  $v_{bc}$  effect is negligible due to the transition to strong stellar feedback.

Comparing the Soft model to the Maximal, with or without  $v_{bc}$ , shows that the main influence of the X-ray spectrum (which affects only the heating fluctuations) is on

the amplitude of the heating peak; in the case of hard X-rays this peak is quite weak, and disappears completely on smaller scales (Fialkov & Barkana 2014). The No-Feedback model artificially keeps low-mass halos forming stars until the end of reionization; the low-redshift normalization thus forces this model to delay its high-redshift SF and related cosmic events. The No-Feedback model is also continuously affected by the streaming velocity, while the other models show a disappearing  $v_{bc}$  effect as reionization ends.

We show in Figure 2 the PS versus  $k$  at several key redshifts. While the overall normalization (which is key for observability) was shown in Figure 1, here we focus on the PS shape (which is key for detecting the  $v_{bc}$  signature). Specifically, we compare the PS at  $k = 0.05 \text{ Mpc}^{-1}$  (the large-scale BAO peak, where the  $v_{bc}$  enhancement is maximized) to its value at  $k = 0.3 \text{ Mpc}^{-1}$  (a scale that is small enough not to be strongly affected by  $v_{bc}$ , yet is large enough compared to our numerical resolution and the angular resolution of observations). We thus examine (at each  $z$ ) the ratio

$$R \equiv \frac{\text{PS}_{v_{bc}}(0.05)}{\text{PS}_{v_{bc}}(0.3)} \left( \frac{\text{PS}_{\text{no-}v_{bc}}(0.05)}{\text{PS}_{\text{no-}v_{bc}}(0.3)} \right)^{-1}, \quad (4)$$

which compares the PS slope with and without  $v_{bc}$ .

The top panel of Figure 2 shows the Ly $\alpha$  peak, the highest-redshift cosmic event with a large 21-cm signal (Barkana & Loeb 2005). At this early time, low-mass halos are likely to dominate, so we compare the Maximal model (with  $f_*(M)$  giving a sharp cutoff) to the Gradual model. As expected, the effect of  $v_{bc}$  is larger for the Maximal model ( $R = 2.2$  compared to  $R = 1.6$ ). Thus, early metal-cooling can enhance the BAO signature at the Ly $\alpha$  peak.

The middle panel highlights the heating peak, showing the strong dependence of this feature on the spectrum of the X-ray heating sources. Hard photons travel further, so the redshifting of the photon energies leads to slower cosmic heating with hard X-rays, as well as smaller fluctuations due to the large-scale smoothing of the heating (Fialkov et al. 2014). The stronger impact of fluctuations (including those

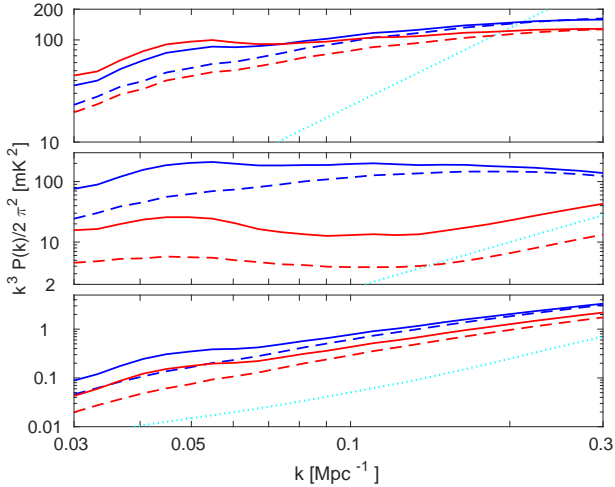


**Figure 2.** The (spherically-averaged) 21-cm power spectrum as a function of  $k$ . We consider different cases at several important redshifts, either with (solid) or without (dashed) the streaming velocity. The top panel focuses on the Ly $\alpha$  peak, and compares the Maximal (red) and Gradual (blue) models. Corresponding redshifts are  $z = 27.4$  (red solid), 29.1 (red dashed), 24.7 (blue solid), and 25.5 (blue dashed). The middle panel focuses on the heating peak, and compares the Maximal (red) and Soft (blue) models. The redshifts are 19.2 (red solid), 19.6 (red dashed), 21 (blue solid), and 22 (blue dashed). The bottom panel shows the midpoint of reionization (i.e., when half the intergalactic medium has been reionized), and compares the Maximal (red) and No-Feedback (blue) models. The redshifts are 10.1 (red solid), 10.6 (red dashed), 8.4 (blue solid), and 8.5 (blue dashed). The cyan dotted line (in each panel) shows the PS of the thermal noise for the SKA1 assuming a single beam, integration time of 1000 hours, and 10 MHz bandwidth at the redshift of the red solid line.

from  $v_{bc}$  in the Soft case (as in Visbal et al. (2012)) yields  $R = 2.9$ , while for the Maximal (hard X-ray) case  $R$  is only 1.4. We note that both cases in this panel assume the sharp  $f_*(M)$  and no LW feedback, features made more likely by the possibility of metal cooling.

The bottom panel shows the possibility of a strong BAO effect from streaming velocity down to relatively low redshift. Specifically, at the midpoint of reionization (a time that current observations are trying to probe), metal cooling may allow a large  $v_{bc}$  effect. Since photoheating feedback is significant at this time, we show the No-Feedback case in addition to the Maximal model. Ionization fluctuations dominate here the 21-cm PS, and the photoheating feedback makes the reionization more spatially uniform since regions with a large ionized fraction experience stronger feedback<sup>2</sup>; it also makes reionization more gradual and thus pushes mid-reionization to a higher redshift relative to the end of reionization. However, due to the continued SF in small halos within the regions that have not yet been reionized, we find only a small effect of this feedback on the power spectrum shape:  $R = 1.8$  for the Maximal model compared with  $R = 2.0$  for the No-Feedback case. We note that in the case of H<sub>2</sub> cooling, LW feedback would have saturated by this

<sup>2</sup> Note that at relatively early times the photoheating feedback can also enhance the fluctuations since it suppresses small galaxies leaving only larger, more highly biased ones.

time (see section 1), giving no  $v_{bc}$  effect (i.e.,  $R = 1$ ), as for the Atomic case.

For the Simulation-Based case, we get  $R = 1.8$  at  $z \sim 14$  (ionization fraction of  $\sim 10\%$ ), while at lower redshifts small halos are significantly suppressed and  $R$  approaches 1.

## 4 SUMMARY AND CONCLUSIONS

In this Letter we have explored the possibility of metal-line cooling in high-redshift low-mass halos, focusing on its effect on the observable 21-cm signal from hydrogen. In the presence of metals, small halos can cool and form stars even after the build-up of the LW background (which shuts down SF via the H<sub>2</sub> cooling channel). Thus, they can continue to contribute to SF even late in cosmic history. Within this scenario we have made predictions for the 21-cm power spectrum from a range of early times ( $z = 6 - 40$ ), accounting for a range of possible parameters for high-redshift astrophysical processes that are poorly constrained at present. In particular, we considered soft or hard SEDs of the first X-ray sources, a sharp or smooth cutoff in the efficiency of SF in low-mass halos, and the effect of ionizing photons on the amount of gas available for cooling (the photoheating feedback).

We found that the SF in small halos, if it is indeed enhanced by metal cooling, can strongly affect the 21-cm signal from all the considered redshifts. An especially interesting implication is that the BAOs imprinted by the supersonic relative velocities between dark matter and baryons on the 21-cm signal, are enhanced and can survive to much later times than previously thought, especially if SF in small halos was more efficient than suggested by current simulations. In particular, the height of the large-scale BAO peak (relative to the PS at smaller scales) is enhanced for our Simulation-Based model by a factor of  $R = 1.8$  down to  $z = 14$  (the beginning of reionization). For the Maximal model the enhancement is by a factor of  $R = 2.2$  at the  $z = 27$  Ly $\alpha$  peak,  $R = 1.4$  at the  $z = 19$  heating peak (boosted to  $R = 2.9$  in the Soft X-ray case), and a still significant  $R = 1.8$  at the midpoint of reionization ( $z = 10$  in this model).

Current experiments are making rapid progress toward detecting the 21-cm signal from  $z \sim 10$ , while future experiments are planned for even higher redshifts. These instruments will likely be able to probe the role of small halos in the history of the early Universe by measuring their 21-cm signature, in particular the BAOs imprinted by the supersonic streaming velocity. Such an exciting detection would shed light on the dawn of star formation.

## 5 ACKNOWLEDGMENTS

We thank L. V. E. Koopmans for providing the noise spectrum of the SKA. R.B. and A.C. acknowledge Israel Science Foundation grant 823/09 and the Ministry of Science and Technology, Israel. A.F. was supported by the LabEx ENS-ICFP: ANR-10-LABX-0010/ANR-10-IDEX-0001-02 PSL. R.B.'s work has been done within the Labex Institut Lagrange de Paris (ILP, reference ANR-10-LABX-63) part of the IDEX SUPER, and received financial state aid managed by the Agence Nationale de la Recherche, as part

of the programme Investissements d'avenir under the reference ANR-11-IDEX-0004-02. R.B. also acknowledges a Levrulme Trust Visiting Professorship.

## REFERENCES

- Ade, P. A. R., et al., 2013, arXiv:1303.5076  
 Ade, P. A. R., et al., 2015, arXiv:1502.01589  
 Ahn, K., Shapiro, P. R., Iliev, I. T., Mellema, G., Pen, U., 2009, ApJ, 695, 1430  
 Ali, Z. S., et al., 2015, arXiv:1502.06016  
 Barkana, R., Loeb, A., 2001, Phys. Rep., 349, 125  
 Barkana, R., Loeb, A. 2005, ApJ, 626, 1  
 Bowman, J. D., et al., 2013, PASA, 30, 31  
 Bromm V., Coppi P. S., Larson R. B., 2002, ApJ, 564, 23  
 Dalal, N., Pen, U.-L., Seljak, U., 2010, JCAP, 11, 007  
 Fialkov, A., Barkana, R., Tseliakhovich, D., Hirata, C. M., 2012, MNRAS, 424, 1335  
 Fialkov, A., Barkana, R., Visbal, E., Tseliakhovich, D., Hirata, C. M., 2013, MNRAS, 432, 2909  
 Fialkov, A., Barkana, R., Visbal, E., 2014, Nature, 506, 197  
 Fialkov, A., Barkana, R., 2014, MNRAS, 445, 213  
 Fialkov, A., 2014, Int. J. Modern Phys. D, 23, 1430017  
 Fragos, T., Lehmer, B. D., Naoz, S., Zezas, A., Basu-Zych, A., 2013, ApJ, 776, 31  
 Furlanetto, S. R., 2006, MNRAS, 371, 867  
 Greif, T., White, S., Klessen, R., Springel, V., 2011, ApJ, 736, 147  
 Haiman, Z., Rees, M. J., Loeb, A., 1997, ApJ, 484, 985  
 Holzbauer L. N., Furlanetto S. R., 2012, MNRAS, 419, 718  
 Jeon, M., Pawlik, A. H., Bromm, V., Milosavljevic, M., 2014, MNRAS, 444, 3288  
 Jeon, M., Bromm, V., Pawlik, A. H., Milosavljevic, M., 2015, MNRAS, 452, 1152  
 Karlsson, T., Bromm, V., Bland-Hawthorn J., 2013, RvMP 85, 809  
 Machacek, M. E., Bryan, G. L., Abel, T., 2001, ApJ, 548, 509  
 Maio, U., Koopmans, L. V. E., Ciardi, B., 2011, MNRAS, 412, L40  
 Mellema G., et al., 2013, ExA, 36, 235  
 Naoz, S., Yoshida, N., Gnedin, N. Y., 2013, ApJ, 763, 27  
 Navarro, J. F., Steinmetz, M. 2000, ApJ, 538, 477  
 O'Leary, R. M., McQuinn, M., 2012, ApJ, 760, 4  
 O'Shea, B. W., Norman, M. L., 2008, ApJ, 673, 14  
 O'Shea, B. W., Wise, J. H., Xu, H., Norman, M. L., 2015, ApJ, 807, 12  
 Pritchard, J. R., Loeb, A., 2008, PRD, 78, 3511  
 Pritchard, J. R., Furlanetto, S. R. 2007, MNRAS, 376, 1680  
 Pritchard, J. R., Loeb, A., 2012, RPP, 75, 6901  
 Rees, M. J. 1986, MNRAS, 222, 27  
 Shi, Y., Armus, L., Helou, G., Stierwalt, S., Gao, Y., Wang, J., Zhang, Z. Y., Gu, Q., 2014, Nature, 514, 335  
 Sobacchi, E., Mesinger, A., 2013, MNRAS, 432, 3340  
 Springel, V., Hernquist, L., 2013, MNRAS, 339, 312  
 Stacy A., Bromm V., Loeb A., 2011, ApJ, 730, 1  
 Tegmark, M., Silk, J., Rees, M., Blanchard, A., Abel, T., Palla, F., 1997, ApJ, 474, 1  
 Tseliakhovich, D., Barkana, R., Hirata, C. M., 2013, MNRAS, 418, 906  
 Tseliakhovich, D., Hirata, C. M., 2010, PRD, 82, 3520  
 van Haarlem, M. P., et al., 2013, A& A, 556, 2  
 Visbal, E., Barkana, R., Fialkov, A., Tseliakhovich, D., Hirata, C. M., 2012, Nature, 487, 70  
 Visbal, E., Haiman, Z., Terrazas, B., Bryan, G. L., Barkana, R., 2014, MNRAS, 442, 100  
 Weinberg, D. H., Hernquist, L., Katz, N. 1997, ApJ, 477, 8  
 Wise, J. H., Abel, T., 2007, ApJ, 671, 1559  
 Wise, J. H., Demchenko, V. G., Halicek, M. T., Norman, M. L., Turk, M. J., Abel, T., Smith, B. D., 2014, MNRAS, 442, 2560  
 Woosley, S. E., Heger, A., 2015, ASSL, 412, 199  
 Yoshida N., Abel T., Hernquist L., Sugiyama, N., 2003, ApJ, 592, 645